ACS OMEGA

http://pubs.acs.org/journal/acsodf

Article

Design, Synthesis, and Bioactivity of Novel Bifunctional Small Molecules for Alzheimer's disease

Meihao Liang, Lili Gu, Hongjie Zhang, Jingli Min, Zunyuan Wang, Zhen Ma, Chixiao Zhang, Shenxin Zeng, Youlu Pan, Dongmei Yan, Zhengrong Shen,* and Wenhai Huang*

Cite This: *ACS Omega* 2022, 7, 26308−26315

Read Online

ACCESS | Metrics & More | Article Recommendations | Supporting Information

ABSTRACT: The abnormal phosphorylation of the τ-protein is a typical early pathological feature of Alzheimer's disease (AD). The excessive phosphorylation of the τ-protein in the brain causes the formation of neurofibrillary tangles (NFTs) and increases the neurotoxicity of amyloid-β (Aβ). Thus, targeting the τ-protein is considered a promising strategy for treating AD. Herein, we designed and synthesized a series of molecules containing bifunctional groups to recognize the τ-protein and the E3 ligase. The molecules were examined *in vitro*, and their effects were tested on PC12 cells. In addition, we further studied the pharmacokinetics of compound I3 in healthy rats. Our data showed that compound I3 could effectively degrade τ-protein, reduce Aβ-induced cytotoxicity, and regulate the uneven distribution of mitochondria, which may open a new therapeutic strategy for the treatment of AD.

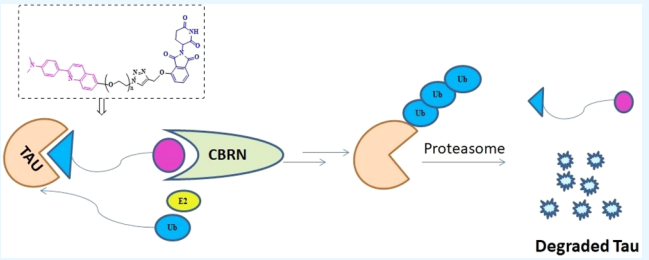

1. INTRODUCTION

Alzheimer's disease (AD) is an irreversible neurodegenerative disease.[1] Abnormal high phosphorylation of the τ-protein is considered an early pathological feature of AD. Excessive phosphorylation of this protein in the brain can induce the formation of neurofibrillary tangles (NFTs) and increase the neurotoxicity of amyloid-β (Aβ), which is positively related to the pathological progress of AD.[2] The pathogenic mechanism of the τ-protein includes two aspects: one is the abnormal phosphorylation of the τ-protein, leading to microtubule depolymerization, and the other is the double-stranded helical filament polymerization-τ (PHF-τ) formed by the aggregation of the τ-protein.[3] Excessive or abnormal phosphorylation leads to microtubule instability, mitochondrial dysfunction, and neurotoxicity. This affects the internal transport of neurotransmitters, induces an inflammatory response, and forms abnormal synapses, thus further promoting the development of AD. Accordingly, the τ-protein has been considered a promising therapeutic target for the treatment of AD.[4]

To date, strategies for treating the τ-protein are mainly based on small-molecule inhibitors,[5,6] traditional Chinese medicine,[7−10] and genetic engineering antibodies.[11] Most candidate inhibitors currently in clinical trials cannot be qualified, since they have pleiotropic activities and exhibit relatively weak biological functions on the τ-protein.[12] Antibodies such as BMS-986168[13] and RO7105705,[14,15] have been investigated; yet, there have been some negative speculations about their pharmacokinetics.

Recently, targeted protein degradation using proteolysis-targeting chimeras (PROTACs) has emerged as an attractive therapeutic modality in drug discovery.[16] PROTACs degrades proteins through the ubiquitin−proteasome system (UPS). First, E1 activates ubiquitin and transfers it to the E2 binding enzyme. E2 ubiquitin-conjugated enzymes are then formed by the reaction of transmercaptan with the E2 conjugate. At the same time, E3 ligase binds to the target protein (POI) and E2 enzymes, enabling ubiquitin to be delivered to the target protein. From there, the proteasome recognizes ubiquitin on the protein and degrades it. PROTACs hijack the inherent intracellular UPS for POI ubiquitination and subsequent proteasome degradation, inducing terpolymer complex (POI−PROTAC−E3 ligase) ubiquitination that leads to target protein destruction. The mechanism of the PROPAC technology[17] is shown in Figure 1. These PROTACs are comprised of three parts: (1) a moiety for recognizing a protein of interest (POI), (2) a moiety for binding to the E3 ligase, and (3) the linker for connecting these ligands. PROTACs can target proteins considered "undruggable" or "indestructible".

Received: April 6, 2022
Accepted: June 24, 2022
Published: July 20, 2022

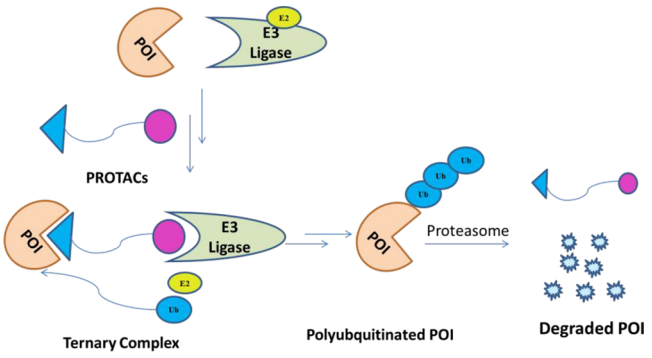

Figure 1. Schematic diagram of PROTACS technology. POI, protein of interest.

With PROTAC technology, more and more POIs such as τ, fibroblast growth factor receptor substrate 2 (FRS2), bromodomain-containing protein 4 (BRD4), estrogen receptor (ER), and methionine aminopeptidase 2 (METAP-2) have been successfully degraded. For example, ARV-471 and ARV-110 (Figure 2A), which target ER and androgen receptor (AR), respectively, have shown promising antitumor activities.[18] Meanwhile, more than 600 types of E3 ligases[19] have been identified. Therein, four E3 ligases, namely, cellular inhibitors of apoptosis 1 (CIAP1),[20] von Hippel Lindau (VHL),[21] cereblon (CRBN),[22] and double mouse minute 2 homologue (MDM2),[23] are mainly used in PROTAC technology. The most commonly used ligands of E3 ligases are shown in Figure 2B.

In 2016, Chen et al.[24] designed and synthesized a peptide Kelch-like ECH associated protein 1 (KEAP1)-CUL3-based PROTAC, named TH006, to degrade the τ-protein via VHL. TH006 can successfully degrade the τ-protein in the animal brain through the ubiquitination system, providing a data basis for the research and development of τ-protein degraders. Two years later, Lu et al.[25] identified Keap1 as a novel candidate for PROTACs that could be applied to degrade the nonenzymatic τ-protein. By applying KEAP1 siRNA and the proteasomal inhibitor MG132, they demonstrated that the τ-degradation of the peptide PROTACs is closely associated with KEAP1 and depends on the ubiquitin-proteasome pathway. However, as a peptide ligand, this strategy has some limitations, including peptide instability, poor blood−brain barrier penetrability, and other drug gability problems.

Okamura et al.[26] discovered a molecular compound THK5105 (labelled ^{18}F) that could specifically bind to the τ-protein in the brain tissue homogenates of AD patients. In this study, we propose using the PROTAC strategy to develop a novel PROTAC for the degradation of the τ-protein. We applied THK5105 as a τ-protein targeting ligand, thalidomide as a recruiting ligand for the E3 ligase, and PEG as the link chain to develop novel bifunctional small-molecule compounds.

2. RESULTS AND DISCUSSION

2.1. Chemistry. The primary role of the τ-protein is to maintain the stability of microtubules in the axon; yet, when the protein is misfolded or abnormal high phosphorylation occurs, the τ-protein can promote the formation of neurofibrillary tangles and induce nerve cell damage and death. Therefore, the development of τ-protein degraders is regarded as a promising approach for anti-AD drug discovery. In this study, a series of novel chimeric molecules with bifunctional groups were synthesized. To achieve satisfying selective recognition and degradation of the τ-protein, the small-molecule probe THK5105 was introduced as the τ-targeted ligand.[27] Thalidomide was chosen as the moiety to recruit E3 ligases, and the two parts were connected by a PEG linker. To improve the synthetic efficiency, we introduced the alkynyl group via the propargyl bromide on the 4-OH of the indole moiety in the thalidomide structure, thus obtaining compound II, as well as the azide group on one end of polyethylene glycol tosylate (Tso-PEG-oTs) via sodium azide, thus obtaining compound III. Through a simple click reaction of compound II with compound III, the final designed compound I (I2−I4) was obtained (Scheme 1).

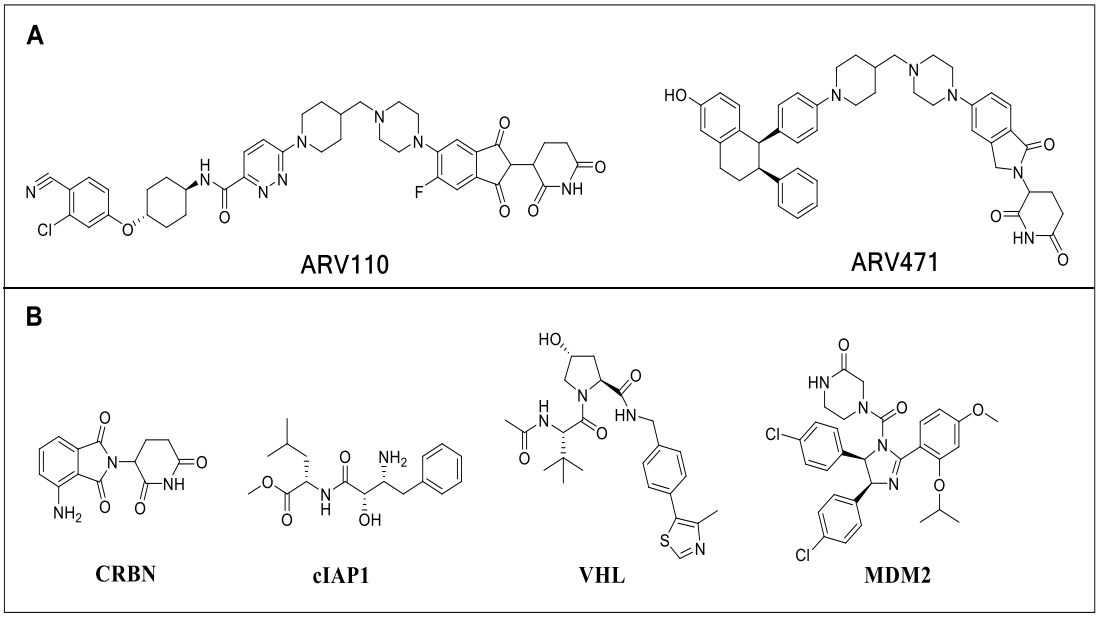

Figure 2. (A) Structures of ARV-110 and ARV-471. (B) Structures of commonly used E3 ligase ligands.

https://doi.org/10.1021/acsomega.2c02130
ACS Omega 2022, 7, 26308−26315

Scheme 1. Synthetic Scheme for Compounds I[a]

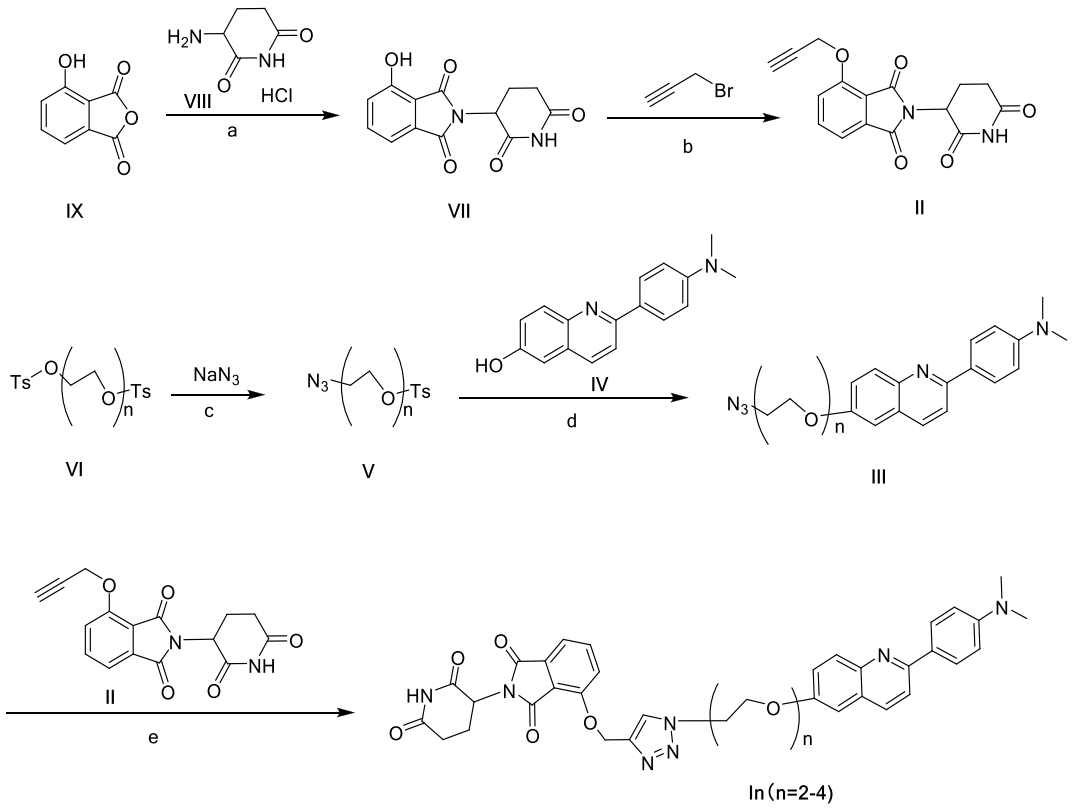

[a]Reagents and conditions are as follows: (a) DMF, 150 °C, 5 h; (b) K_2CO_3, DMF, 60 °C; (c) DMF, 40 °C, 4 h; (d) K_2CO_3, DMF, 60 °C; and (e) N_2, rt, 24 h.

2.2. Morphological Observation. The PC12 cell line is one of the most commonly used cell lines in neuroscience research, including studies of neurotoxicity, neuroprotection, neurosecretion, neuroinflammation, and synaptogenesis.[28] We first investigated the morphological effects of the new compounds on the PC12 cells. After the PC12 cells were treated with I2−I4 (10 μM) for 24 h, no significant morphological changes were observed (Figure 3), which indicated that compounds I2−I4 were not toxic to the cells.

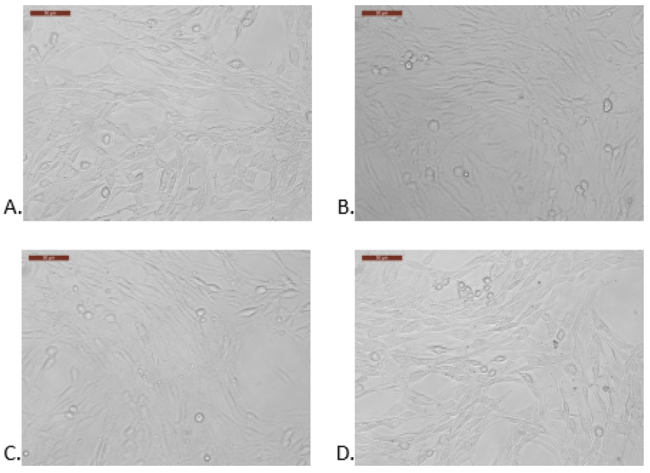

Figure 3. Effects of compounds on cell morphology (×200). (A) Blank. (B) I2 (10 mM for 24h). (C) I3 (10 μM for 24h). (D) I4 (10 μM for 24h).

2.3. Degradation of the τ-Protein. To investigate the degradation ability of compounds I2−I4 with regard to the τ-protein, PC12 cells were treated with I2, I3, or I4 for 24 h. Cells were then lysed, and the total proteins were analyzed by Western blot. As shown in Figure 4, I2−I4 could reduce the

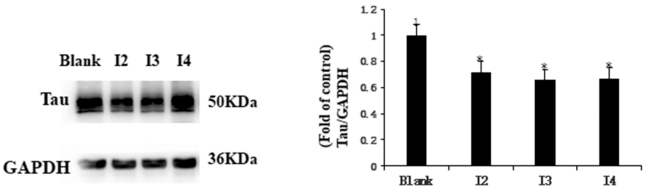

Figure 4. τ-Protein expression in PC12 cells treated with I2−I4 (10 μM) for 24 h. Data were analyzed by Western blot. GAPDH was used as a loading control. *P < 0.05 vs the control group.

expression of endogenous τ-protein in PC12 cells at a concentration of 10 μM compared to a normal group (P < 0.05). The degradation abilities of compounds I2−I4 are similar.

2.4. τ-Degradation is Dose- and Time-Dependent. We further assessed the dose- and time degradation profiles of τ-degradation. When PC12 cells were treated with increasing doses of I3 (from 12.5 to 200 μM) for 24 h, the level of the τ-protein gradually decreased in a dose-dependent manner (Figure 5A); the statistical difference between testing and control cells was seen after concentrations of 25 μM and above were applied.

https://doi.org/10.1021/acsomega.2c02130
ACS Omega 2022, 7, 26308−26315

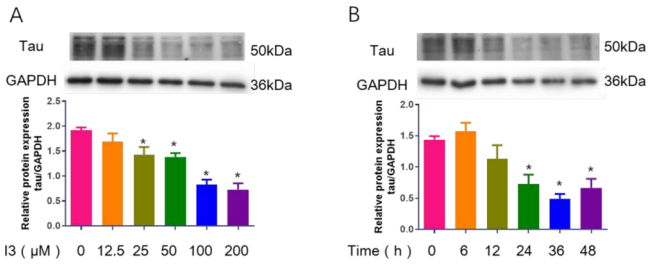

Figure 5. τ-Protein degradation in PC12 cells treated with I3. Data were analyzed by Western blot. (A) PC12 cells treated with increasing amounts of I3 for 24 h. (B) PC12 cells treated with 50 μM I3 for 0, 6, 12, 24, 36, and 48 h. GAPDH was used as a loading control. *$P < 0.05$ vs the control group.

PC12 cells were treated with 50 μM I3 for 0, 6, 12, 24, 36, and 48 h. As shown in Figure 5B, the level of the τ-protein gradually decreased in a time-dependent manner; the statistical difference between the testing and control cells was seen after 24 h.

2.5. τ-Degradation via the Proteasome Pathway. We further tested whether I3 promoted τ-degradation via a polyubiquitination system. The proteasome inhibitor MG132 and the autophagy inhibitor bafilomycin A1 (BA) were separately used to disturb major protein degradation routes, namely, the proteasome pathway and the autophagy pathway, respectively. As shown in Figure 6, when MG132 or BA was

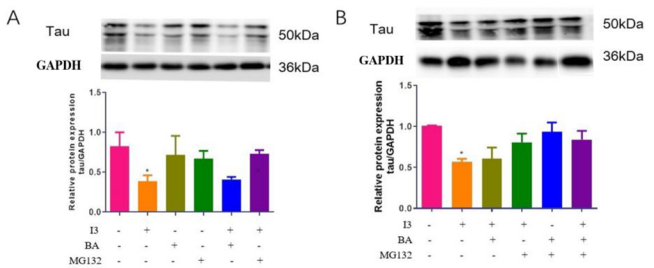

Figure 6. (A and B) τ-Protein levels in PC12 cells treated with I3 (50 μM) combined with MG132 (4 mM) and bafilomycin A1 (0.4 mM), respectively. Data were analyzed by Western blot. GAPDH was used as a loading control. *$P < 0.05$ vs the control group ($n = 3$).

used alone, there was no significant difference in τ-protein expression in comparison with that in normal controls ($P > 0.05$). It was suspected that blocking the ubiquitin−proteasome system with MG132 might activate other pathways to degrade τ-protin.[29] In addition, no change in τ-protein expression was found in the MG132+I3 cotreatment group. Yet, the level of τ-protein was significantly down-regulated in the BA+I3 cotreatment group ($P < 0.05$), which indicated that the induction of τ-degradation by I3 could be depressed by MG132. This further suggested that the I3 induced τ-degradation via the polyubiquitination pathway.

2.6. Rescuing the Uneven Distribution of Mitochondria. τ-Protein overexpression affects cell morphology, including uneven mitochondrial distribution.[30] Thus, green fluorescent protein-τ (GFP-τ) was transferred into the PC12 cells and used to investigate the ability of compound I3 to rescueuneven mitochondria distribution. As shown in Figure 7, the mitochondria of cells with τ-overexpression tend to cluster on one side of the nucleus. However, after the I3 treatment, the mitochondria of τ-overexpressed cells were more evenly

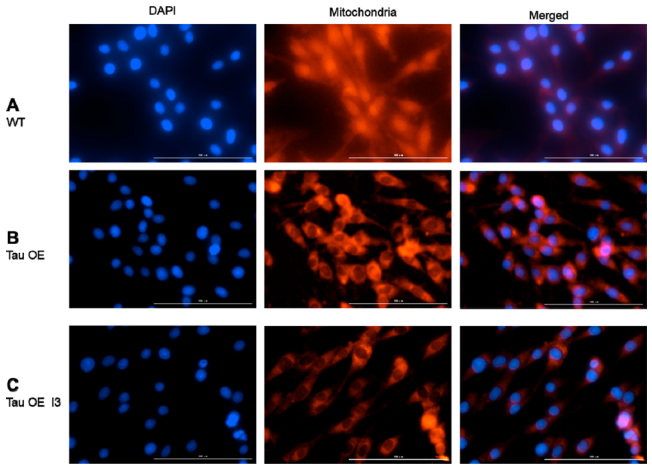

Figure 7. Microscopic images show the distribution of mitochondria in (A) wild-type cells, (B) untreated τ-protein overexpressing cells, and (C) τ-protein overexpressing cells treated with 50 μM I3 for 24 h. The first column shows DAP0 stained nuclei (blue), the second column shows mitochondria (red) labeled with Mito Tracker Red, and the third column shows the merged images. The scale bar represents 100 μm.

distributed in the whole cytoplasm. The results suggested that the partial degradation of intracellular τ-protein could improve the uneven distribution of mitochondria.

2.7. Reducing the Toxicity of Aβ. Excessive phosphorylation of the τ-protein in the brain increases the neurotoxicity of Aβ.[31] Thus, in this study, we used the MTT assay to evaluate the potential of compound I3 to reduce the toxicity of Aβ. The effect of compound I3 on cell viability was first examined. As shown in Figure 8A, compound I3 (<200 μM) had no significant effect on cell viability; yet, when the concentration of compound I3 reached 200 μM, the survival rate of the PC12 cells significantly decreased ($P < 0.05$). Compound I3 (<100 μM) was then cotreated with Aβ1−42 (10 μM). Compared with the Aβ1−42 treatment group, compound I3 increased the cell survival rate at a dosage of 6.25−12.5 mM (Figure 8B). This suggests that the τ-protein has a certain role in stabilizing cell activity; if it is excessively degraded, it will be detrimental to and decrease cell activity. There was a significant difference ($P < 0.05$) between the 12.5 μM group and the Aβ1−42 treatment group, suggesting that compound I3 can reduce the cytotoxicity induced by Aβ1−42. These results demonstrated that I3 could partially counteract the toxicity of Aβ1−42 by lowering intracellular τ-levels in wild-type PC12. The results also support the hypothesis that compound I3 has excellent membrane permeability.

2.8. Pharmacokinetics Characteristics of I3. We further studied the pharmacokinetics of compound I3 in healthy rats at a dose of 30 mg/kg (po). The concentrations of compound I3 in the brain and plasma were determined by liquid chromatography-tandem mass spectrometric (LC/MS). After administration, the peak concentration in the brain (C_{max} = 29.10 ng/mL) was higher than that in the plasma (C_{max} = 18.03 ng/mL) (Figure 9). Compound I3 was deemed "brain penetrant" due to its brain-to-plasma concentration ratio (C_b:C_p) >1.60.

3. CONCLUSION

Our data showed compound I3 could effectively degrade τ-protein in PC12 cells, reduce Aβ-induced cytotoxicity and

https://doi.org/10.1021/acsomega.2c02130
ACS Omega 2022, 7, 26308−26315

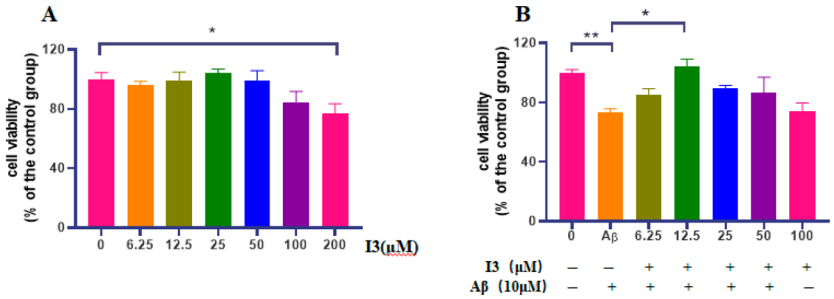

Figure 8. I3 reduces the toxicity of Aβ. Plots of (A) the toxicity of I3 to PC12 cells and (B) the cell viability of PC12 cells treated with Aβ (10 μM) or Aβ in combination with I3. Data are means ± SEM, n = 5. *P < 0.05 and **P < 0.01.

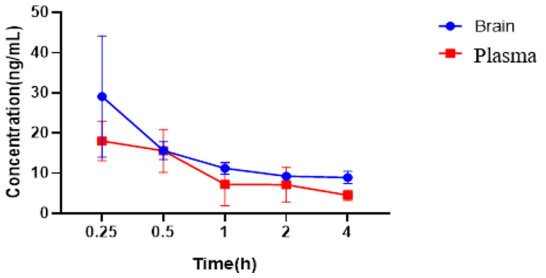

Figure 9. Brain and plasma drug concentration−time curve (mean ± SEM, n = 3) after oral administration of 30 mg/kg of I3 in rats.

regulate the uneven distribution of mitochondria, which may lead to important advancements in AD drug development.

4. EXPERIMENTAL SECTION

4.1. Materials and Methods. All the used solvents were of analytical grade. ^{1}H NMR spectra were recorded on a Bruker Avance III 400 M instrument (chemical shifts were expressed as δ values relative to TMS as the internal standard). High-resolution mass spectra (HRMS) were recorded on a Waters Synapt G2 spectrometer. Mass spectra (MS) was recorded on a Acquity Qda/TLC MS Interface2 spectrometer. LC/MS spectra were recorded on a Fisherinstrument. Column chromatography was conducted on a column of silica gel (200−300 mesh).

4.1.1. 2-(2,6-Dioxo-piperidin-3-yl)-4-hydroxy-isoindole-1,3-dione (VII). Compound VIII (3.2 g, 19.5 mmol) and compound IX (2.8 g, 19.8 mmol) were dissolved in dimethylformamide (DMF), and the mixture was placed in a 150 °C oil bath for 5 h. After the mixture was cooled, filtrated, and washed with ethyl acetate (EA), the solid layer was dried to obtain compound VII (4.5 g, 84.3%). MS calcd. for $C_{13}H_{11}N_2O_5$ $[M + H]^+$: 275.06. Found: 275.23.

4.1.2. (2-Oxo-piperidin-3-yl)-4-prop-2-ynyloxy-isoindole-1,3-dione (II). Compound VII (2.0 g, 7.3 mmol) and 3-bromo-1-propyne were first dissolved in DMF, and the solution was mixed with potassium carbonate (1.2 g, 8.7 mmol). The reaction mixture was stirred at room temperature for 5 h. After that, the aqueous solution was extracted by EA. After the mixture was washed with saturated sodium chloride and dried over Na_2SO_4, EA was removed, and compound II (2.0 g, 83.3%) was obtained. HRMS calcd. for $C_{16}H_{13}N_2O_5$ $[M + H]^+$: 335.0746. Found: 335.0630.

4.1.3. Toluene-4-sulfonic Acid 2-{2-[2-(Triazirin-1-yloxy)-ethoxy]-ethoxy}-ethyl Ester (V1−V3). Taking V3 as an example, triethylene glycol di-p-toluene sulfonic acid (VI3) (0.5 g, 1.1 mmol) and sodium azide (0.04 g, 1.1 mmol) were dissolved in DMF. Afterward, the mixture was stirred at 40 °C and monitored by TLC. After the reaction was complete, water was added, and the mixture was extracted with EA. After the mixture was dried over Na_2SO_4, EA was removed, and compound V3 (0.35 g, 85.4%) was obtained. MS calcd. for $C_{13}H_{20}N_3O_5S$ $[M + H]^+$: 330.10. Found: 330.15.

4.1.4. Dimethyl-{4-[6-(2-{2-[2-(triazirin-1-yloxy)-ethoxy]-ethoxy}-ethoxy)-quinolin- 2-yl]-phenyl}-amine (III3). Taking III3 as an example, compound V3 (0.19 g, 0.51 mmol), compound IV (0.14 g, 0.61 mmol), and K_2CO_3 (0.08 g, 0.58 mmol) were dissolved in DMF. The reaction was performed for 5 h at 60 °C. After the reaction was complete, water was added, and the mixture was extracted with EA. After the mixture was dried over Na_2SO_4, EA was removed, and compound III3 (0.16 g, 76.2%) was obtained. MS calcd. for $C_{23}H_{27}N_5O_3$ $[M + H]^+$: 422.21. Found: 422.17.

4.1.5. General Procedure A for the Syntheses of Compounds I2−I4. Taking I3 as an example, compound III3 (0.12 g, 0.28 mmol), compound II (0.09 g, 0.28 mmol), copper sulfate (9.2 mg, 0.06 mmol), and vitamin C sodium (11.2 mg, 0.06 mmol) were dissolved in DMF. The mixture was stirred for 24 h at room temperature. The aqueous solution was then extracted by EA and washed with water. After the mixture was dried over Na_2SO_4, EA was removed, and compound I3 (0.11 g, yield 55.02%) was obtained. ^{1}H NMR (400 MHz, DMSO-d_6) δ 7.88 (s, 1H, ArH), 7.86 (m, 2H, ArH), 7.84 (s, 2H, ArH), 7.63 (m, 1H, ArH), 7.58 (s, 2H, ArH), 7.58 (s, 2H, ArH), 7.31 (s, 1H, ArH), 7.21 (d, 1H, ArH), 5.13 (m, 2H, CH_2), 5.07 (t, 1H, CH), 3.70 (m, 4 H, CH_2), 2.85−2.94 (m, 4 H, CH_2), 2.79 (s, 6H, $(CH_3)_2$), 2.47−2.62 (m, 2H, CH_2), 2.02−2.11 (m, 4 H, CH_2). HRMS calcd. for $C_{39}H_{40}N_7O_8$ $[M + H]^+$: 734.2860. Found: 734.2952.

4.1.6. 4-[1-(2-{2-[2-(4-Dimethylamino-phenyl)-quinolin-6-yloxy]-ethoxy}-ethyl)-4,5-dihydro-1H-[1,2,3]triazol-4-ylmethoxy]-2-(2,6-dioxo-piperidin-3-yl)-isoindole-1,3-dione (I2). Compound I2 was obtained from compound III2 and compound II following general procedure A (27.0 mg, yield 20.4%). ^{1}H NMR (400 MHz, DMSO-d_6) δ 8.14 (d, 2H, ArH), 7.71−7.75 (m, 4H, ArH), 7.52−7.54 (d, 2H, ArH), 7.40−7.42 (m, 4H, ArH), 4.97 (m, 2H, CH_2O), 4.10−4.15 (q, 3H, CHN, CH_2O), 2.79−2.85 (m, 6H, 3-CH_2O), 2.59−2.79 (s, 6H, 2(−CH_3N)), 2.21−2.20 (m, 4H, 2(−CH_2C)). HRMS calcd. for $C_{37}H_{38}N_7O_7$ $[M + H]^+$: 690.2712. Found: 690.2687.

4.1.7. 4-[1-(2-{3-[2-(4-Dimethylamino-phenyl)-quinolin-6-yloxy]-propoxy}-ethyl)-4,5-dihydro-1H-[1,2,3]triazol-4-ylmethoxy]-2-(2,6-dioxo-piperidin-3-yl)-isoindole-1,3-dione (I4). Compound I4 was obtained from compound III4 and compound II following general procedure A (41.0 mg, yield 17.9%). ^{1}H NMR (400 MHz, DMSO-d_6) δ 8.42 (t, 1H, ArH),

https://doi.org/10.1021/acsomega.2c02130
ACS Omega 2022, 7, 26308−26315

8.03 (s, 1H, ArH), 7.94 (d, 1H, ArH), 7.8 (m, 4H, ArH), 7.52 (dd, 0.5H, ArH), 7.33 (m, 4H, ArH), 7.25 (s, 0.5H, ArH), 4.09−4.33 (m, 3H, −CHN, $-CH_2$), 3.57−3.6 (m, 14H, 7($-CH_2O$)), 2.90−3.18 (s, 6H, 2($-CH_3N$)), 1.39 (m, 4H, 2($-CH_2C$)). HRMS calcd. for $C_{41}H_{46}N_7O_9$ $[M + H]^+$: 778.3279. Found: 778.3717.

4.2. *In Vitro* Experiments. *4.2.1. Cells.* PC12 cells (rat pheochromocytoma cells) were obtained from the Cell Center of the Chinese Academy of Medical Sciences (Beijing, China). PC12 cells were cultured in DMEM (Tianhang, China), supplemented with 10% FBS and 1% penicillin/streptomycin, and incubated in a humidified atmosphere containing 5% CO_2 and 95% air at 37 °C (NuAire auto flow IR direct heat CO_2 incubator, model no. NU-5510E).

4.2.2. Morphological Observation. The PC12 cells (1×10^6/well) were cultured in 2 mL of the medium in 6-well plates for 24 h. Cells were divided into four groups: the blank group and I2, I3, and I4 groups. The morphological changes of cells were recorded using a microscope (Leica DMI3000B). The complete experimental procedure was performed according to ref 32.

4.2.3. Western Blot. The PC12 cells (1×10^6/well) were cultured in 2 mL of the medium in 6-well plates and then treated with I2, I3, and I4. After 24 h of incubation, the cells were lysed, and the total protein was extracted and denaturated at 100 °C for 5 min. The protein (20 μg) was collected. Electrophoresis was performed using SDS-PAGE at 80 V and 200 mA for 100 min. The membrane was transferred and sealed at room temperature for 1 h. The membrane was incubated first with the corresponding primary antibodies, namely τ (dilution ratio of 1:1000, Biyuntian, AF1249) and glyceraldehyde-3-phosphate dehydrogenase (GAPDH) (dilution ratio of 1:2000, rabbit anti-GAPDH, AB-P-R 001, Goodhere, China), at 4 °C overnight and then with the corresponding secondary antibodies (dilution ratio of 1:2000, antirabbit IgG HRP-linked antibody, CST no. 7074S) at room temperature for 2 h. A gel imaging system ECL (Amersham Imagequant 800, Japan) was used for image acquisition, and the relative gray value of the protein was analyzed. The complete experimental procedure was performed according ref 33.

4.2.4. Mitochondrial Morphology Observation. PC12 cells were seeded in a 12-well plate at a density of 5×10^5 cells per well in 1 mL of the medium. After reaching 30−50% confluence, cells were transfected with pcDNA-GFP-τ (accession no. NM_001123066.3) using the Lipo6000 transfection reagent (Biyuntian, C0526) following the manufacturer's instructions. After 24 h, the medium was removed, cells were washed with PBS, and 1 mL of the medium containing Mito Tracker Red CMXROS (mitochondrial red fluorescent probe, Biyuntian, C1035) was added to the culture for 25 min. The medium was then removed, and the cells were sealed with an antifluorescence quenching solution containing DAPI (Biyuntian, P0131) and analyzed using a fluorescence microscope. The complete experimental procedure was performed according to ref 25.

4.2.5. MTT Assay. PC12 cells in the logarithmic phase were seeded in a 96-well plate at a density of 1×10^4 cells per well in 100 μL of media containing various concentrations of I3 or $A\beta_{1-42}$. After 24 h, 20 μL of sterile MTT dye (5 mg/mL, Biyuntian, ST316) was added to each well, and culteres incubated for another 4 h at 37 °C. After the medium was removed, 150 μL of DMSO was added to each well and properly mixed for another 10 min. The absorbance at 570 nm was determined using a microplate reader (Bio-Tek Cytation 1). IC_{50} values were calculated from the linear regression of the plot. The experimental procedure was performed according to ref 34.

4.3. Animals and Pharmacokinetics (PK) Study. ICR male nude mice, 6−8 weeks old, were obtained from Zhejiang Animal Center (Hangzhou, China). All the animals were housed in an environment with a temperature of 22 ± 1 °C, a relative humidity of 50 ± 1%, and a light−dark cycle of 12−12 h. All the animal studies were approved by the Ethical Committee of Hangzhou Medical College according to the recommendations in the Guide for the Care and Use of Laboratory Animals.

Compound I3 was diluted with DMSO at a concentration of 1 mg/mL. The nine ICR male nude mice (male, 8 weeks) were randomly divided into three groups (3 mice per group). After the mice were fasted for 12 h, baseline blood was collected into a tube containing 20 μL of EDTA (1 mg/mL). Animals were then treated with intragastric (po) administration (30 mg/kg). Subsequently, blood and brains were extracted from each animal. Blood was collected at 0, 0.25, 0.5, 1, 2, and 4 h. All blood was immediately centrifuged at 4000 rpm for 10 min, then the plasma and brains were harvested and stored at −80 °C in the special refrigerator prior to analysis. The supernatant from the samples was separated and analyzed using LC/MS. The complete experimental procedure is described in our previous publication.[35]

4.4. Statistical Analysis. Unless otherwise indicated, all the data are presented as the mean ± SEM. The statistical significance of the differences between two groups was analyzed using Student's *t* test. A p-value of <0.05 was considered to be statistically significant.

■ ASSOCIATED CONTENT

Supporting Information

The Supporting Information is available free of charge at https://pubs.acs.org/doi/10.1021/acsomega.2c02130.

Compound characterization, NMR spectra, and MS spectra (PDF)

■ AUTHOR INFORMATION

Corresponding Authors

Zhengrong Shen − *Key Laboratory of Neuropsychiatric Drug Research of Zhejiang Province, School of Pharmacy, Hangzhou Medical College, Hangzhou, Zhejiang 310013, P.R. China*; Email: shenzr601@163.com

Wenhai Huang − *Affiliated Yongkang First People's Hospital and School of Pharmacy, Hangzhou Medical College, Hangzhou, Zhejiang 310013, China; Key Laboratory of Neuropsychiatric Drug Research of Zhejiang Province, School of Pharmacy, Hangzhou Medical College, Hangzhou, Zhejiang 310013, P.R. China*; Email: cyj@zju.edu.cn

Authors

Meihao Liang − *Affiliated Yongkang First People's Hospital and School of Pharmacy, Hangzhou Medical College, Hangzhou, Zhejiang 310013, China; Key Laboratory of Neuropsychiatric Drug Research of Zhejiang Province, School of Pharmacy, Hangzhou Medical College, Hangzhou, Zhejiang 310013, P.R. China*

https://doi.org/10.1021/acsomega.2c02130
ACS Omega 2022, 7, 26308−26315

Lili Gu − *Key Laboratory of Neuropsychiatric Drug Research of Zhejiang Province, School of Pharmacy, Hangzhou Medical College, Hangzhou, Zhejiang 310013, P.R. China*
Hongjie Zhang − *Key Laboratory of Neuropsychiatric Drug Research of Zhejiang Province, School of Pharmacy, Hangzhou Medical College, Hangzhou, Zhejiang 310013, P.R. China*
Jingli Min − *Key Laboratory of Neuropsychiatric Drug Research of Zhejiang Province, School of Pharmacy, Hangzhou Medical College, Hangzhou, Zhejiang 310013, P.R. China*
Zunyuan Wang − *Key Laboratory of Neuropsychiatric Drug Research of Zhejiang Province, School of Pharmacy, Hangzhou Medical College, Hangzhou, Zhejiang 310013, P.R. China*
Zhen Ma − *Key Laboratory of Neuropsychiatric Drug Research of Zhejiang Province, School of Pharmacy, Hangzhou Medical College, Hangzhou, Zhejiang 310013, P.R. China*
Chixiao Zhang − *Key Laboratory of Neuropsychiatric Drug Research of Zhejiang Province, School of Pharmacy, Hangzhou Medical College, Hangzhou, Zhejiang 310013, P.R. China*
Shenxin Zeng − *Key Laboratory of Neuropsychiatric Drug Research of Zhejiang Province, School of Pharmacy, Hangzhou Medical College, Hangzhou, Zhejiang 310013, P.R. China*
Youlu Pan − *Key Laboratory of Neuropsychiatric Drug Research of Zhejiang Province, School of Pharmacy, Hangzhou Medical College, Hangzhou, Zhejiang 310013, P.R. China*
Dongmei Yan − *Key Laboratory of Neuropsychiatric Drug Research of Zhejiang Province, School of Pharmacy, Hangzhou Medical College, Hangzhou, Zhejiang 310013, P.R. China*

Complete contact information is available at: https://pubs.acs.org/10.1021/acsomega.2c02130

Notes

The authors declare no competing financial interest.

■ ACKNOWLEDGMENTS

This research was supported by the Huadong Medicine Joint Funds of the Zhejiang Provincial Natural Science Foundation of China under Grant HDMD22H308211, the Zhejiang Provincial Key Research and Development Plan (2021C03083), the Health and Family Planning Commission of Zhejiang Province (XKQ-010-001 and 2021KY630), and the Key Laboratory Of Neuropsychiatric Drug Research of Zhejiang Province (2019E10021).

■ ABBREVIATIONS

AD, Alzheimer's disease; NFT, neurofibrillary tangle; Aβ, amyloid-β; PHF-τ, helical filament polymerization-τ; DMEM, Dulbecco's modified Eagle's medium; PBS, phosphate-buffered saline

■ REFERENCES

(1) Probst, A.; Langui, D.; Ulrich, J. Alzheimer's disease: a description of the structural lesions. *Brain Pathol* **1991**, *1* (4), 229−39.
(2) Zeng, Y.; Yang, J.; Zhang, B.; Gao, M.; Su, Z.; Huang, Y. The structure and phase of tau: from monomer to amyloid filament. *Cell. Mol. Life Sci.* **2021**, *78* (5), 1873−1886.
(3) Brendel, M.; Jaworska, A.; Probst, F.; Overhoff, F.; Korzhova, V.; Lindner, S.; Carlsen, J.; Bartenstein, P.; Harada, R.; Kudo, Y.; Haass, C.; Van Leuven, F.; Okamura, N.; Herms, J.; Rominger, A. Small-Animal PET Imaging of Tau Pathology with 18F-THK5117 in 2 Transgenic Mouse Models. *J. Nucl. Med.* **2016**, *57* (5), 792−8.
(4) Bretteville, A.; Planel, E. Tau aggregates: toxic, inert, or protective species? *J. Alzheimers Dis* **2008**, *14* (4), 431−6.
(5) Ingham, D. J.; Blankenfeld, B. R.; Chacko, S.; Perera, C.; Oakley, B. R.; Gamblin, T. C. Fungally Derived Isoquinoline Demonstrates Inducer-Specific Tau Aggregation Inhibition. *Biochemistry* **2021**, *60* (21), 1658−1669.
(6) Riedel, G.; Klein, J.; Niewiadomska, G.; Kondak, C.; Schwab, K.; Lauer, D.; Magbagbeolu, M.; Steczkowska, M.; Zadrozny, M.; Wydrych, M.; Cranston, A.; Melis, V.; Santos, R. X.; Theuring, F.; Harrington, C. R.; Wischik, C. M. Mechanisms of Anticholinesterase Interference with Tau Aggregation Inhibitor Activity in a Tau-Transgenic Mouse Model. *Curr. Alzheimer Res.* **2020**, *17* (3), 285−296.
(7) Sreenivasmurthy, S. G.; Iyaswamy, A.; Krishnamoorthi, S.; Senapati, S.; Malampati, S.; Zhu, Z.; Su, C. F.; Liu, J.; Guan, X. J.; Tong, B. C.; Cheung, K. H.; Tan, J. Q.; Lu, J. H.; Durairajan, S. S. K.; Song, J. X.; Li, M. Protopine promotes the proteasomal degradation of pathological tau in Alzheimer's disease models via HDAC6 inhibition. *Phytomedicine* **2022**, *96*, 153887.
(8) Iyaswamy, A.; Krishnamoorthi, S. K.; Zhang, H.; Sreenivasmurthy, S. G.; Zhu, Z.; Liu, J.; Su, C. F.; Guan, X. J.; Wang, Z. Y.; Cheung, K. H.; Song, J. X.; Durairajan, S. S. K.; Li, M. Qingyangshen mitigates amyloid-beta and Tau aggregate defects involving PPARalpha-TFEB activation in transgenic mice of Alzheimer's disease. *Phytomedicine* **2021**, *91*, 153648.
(9) Iyaswamy, A.; Wang, X.; Krishnamoorthi, S.; Kaliamoorthy, V.; Sreenivasmurthy, S. G.; Kumar Durairajan, S. S.; Song, J. X.; Tong, B. C.; Zhu, Z.; Su, C. F.; Liu, J.; Cheung, K. H.; Lu, J. H.; Tan, J. Q.; Li, H. W.; Wong, M. S.; Li, M. Theranostic F-SLOH mitigates Alzheimer's disease pathology involving TFEB and ameliorates cognitive functions in Alzheimer's disease models. *Redox Biol.* **2022**, *51*, 102280.
(10) Iyaswamy, A.; Krishnamoorthi, S. K.; Liu, Y. W.; Song, J. X.; Kammala, A. K.; Sreenivasmurthy, S. G.; Malampati, S.; Tong, B. C. K.; Selvarasu, K.; Cheung, K. H.; Lu, J. H.; Tan, J. Q.; Huang, C. Y.; Durairajan, S. S. K.; Li, M. Yuan-Hu Zhi Tong Prescription Mitigates Tau Pathology and Alleviates Memory Deficiency in the Preclinical Models of Alzheimer's Disease. *Front Pharmacol* **2020**, *11*, 584770.
(11) Monteiro, K. L. C.; Alcantara, M.; de Aquino, T. M.; da Silva-Junior, E. F. Tau protein Aggregation in Alzheimer's Disease: Recent Advances in the Development of Novel Therapeutic Agents. *Curr. Pharm. Des* **2020**, *26* (15), 1682−1692.
(12) Chong, F. P.; Ng, K. Y.; Koh, R. Y.; Chye, S. M. Tau proteins and Tauopathies in Alzheimer's Disease. *Cell Mol. Neurobiol* **2018**, *38* (5), 965−980.
(13) Ondrus, M.; Novak, P. Design of the phase II clinical study of the tau vaccine AADvac1 in patients with mild Alzheimer's disease. *Neurobiol. Aging* **2016**, *39*, S26.
(14) Lee, S.-H.; Le Pichon, C. E.; Adolfsson, O.; Gafner, V.; Pihlgren, M.; Lin, H.; Solanoy, H.; Brendza, R.; Ngu, H.; Foreman, O.; Chan, R.; Ernst, J. A.; DiCara, D.; Hotzel, I.; Srinivasan, K.; Hansen, D. V.; Atwal, J.; Lu, Y.; Bumbaca, D.; Pfeifer, A.; Watts, R. J.; Muhs, A.; Scearce-Levie, K.; Ayalon, G. Antibody-Mediated Targeting of Tau In Vivo Does Not Require Effector Function and Microglial Engagement. *Cell Reports* **2016**, *16* (6), 1690−1700.
(15) Ising, C.; Gallardo, G.; Leyns, C. E. G.; Wong, C. H.; Jiang, H.; Stewart, F.; Koscal, L. J.; Roh, J.; Robinson, G. O.; Remolina Serrano, J.; Holtzman, D. M. AAV-mediated expression of anti-tau scFvs decreases tau accumulation in a mouse model of tauopathy. *J. Exp Med.* **2017**, *214* (5), 1227−1238.

(16) Dale, B.; Cheng, M.; Park, K. S.; Kaniskan, H. U.; Xiong, Y.; Jin, J. Advancing targeted protein degradation for cancer therapy. *Nat. Rev. Cancer* **2021**, *21* (10), 638−654.
(17) Lai, A.; Kahraman, M.; Govek, S.; Nagasawa, J.; Bonnefous, C.; Julien, J.; Douglas, K.; Sensintaffar, J.; Lu, N.; Lee, K. J.; Aparicio, A.; Kaufman, J.; Qian, J.; Shao, G.; Prudente, R.; Moon, M. J.; Joseph, J. D.; Darimont, B.; Brigham, D.; Grillot, K.; Heyman, R.; Rix, P. J.; Hager, J. H.; Smith, N. D. Identification of GDC-0810 (ARN-810), an Orally Bioavailable Selective Estrogen Receptor Degrader (SERD) that Demonstrates Robust Activity in Tamoxifen-Resistant Breast Cancer Xenografts. *J. Med. Chem.* **2015**, *58* (12), 4888−904.
(18) Garner, F.; Shomali, M.; Paquin, D.; Lyttle, C. R.; Hattersley, G. RAD1901: a novel, orally bioavailable selective estrogen receptor degrader that demonstrates antitumor activity in breast cancer xenograft models. *Anticancer Drugs* **2015**, *26* (9), 948−956.
(19) Wang, M.; Dai, W.; Ke, Z.; Li, Y. Functional roles of E3 ubiquitin ligases in gastric cancer (Review). *Oncol. Lett.* **2020**, *20* (4), 22.
(20) Lala-Tabbert, N.; Lejmi-Mrad, R.; Timusk, K.; Fukano, M.; Holbrook, J.; St-Jean, M.; LaCasse, E. C.; Korneluk, R. G. Targeted ablation of the cellular inhibitor of apoptosis 1 (cIAP1) attenuates denervation-induced skeletal muscle atrophy. *Skelet Muscle* **2019**, *9*, 13.
(21) Zoppi, V.; Hughes, S. J.; Maniaci, C.; Testa, A.; Gmaschitz, T.; Wieshofer, C.; Koegl, M.; Riching, K. M.; Daniels, D. L.; Spallarossa, A.; Ciulli, A. Iterative Design and Optimization of Initially Inactive Proteolysis Targeting Chimeras (PROTACs) Identify VZ185 as a Potent, Fast, and Selective von Hippel-Lindau (VHL) Based Dual Degrader Probe of BRD9 and BRD7. *J. Med. Chem.* **2019**, *62* (2), 699−726.
(22) Steinebach, C.; Lindner, S.; Udeshi, N. D.; Mani, D. C.; Kehm, H.; Köpff, S.; Carr, S. A.; Gütschow, M.; Krönke, J. Homo-PROTACs for the Chemical Knockdown of Cereblon. *ACS Chem. Biol.* **2018**, *13* (9), 2771−2782.
(23) Winship, A.; Ton, A.; Van Sinderen, M.; Menkhorst, E.; Rainczuk, K.; Griffiths, M.; Cuman, C.; Dimitriadis, E. Mouse double minute homologue 2 (MDM2) downregulation by miR-661 impairs human endometrial epithelial cell adhesive capacity. *Reprod. Fertil. Dev.* **2018**, *30* (3), 477−486.
(24) Chu, T.-T.; Gao, N.; Li, Q.-Q.; Chen, P.-G.; Yang, X.-F.; Chen, Y.-X.; Zhao, Y.-F.; Li, Y.-M. Specific Knockdown of Endogenous Tau Protein by Peptide-Directed Ubiquitin-Proteasome Degradation. *Cell Chemical Biology* **2016**, *23* (4), 453−461.
(25) Lu, M.; Liu, T.; Jiao, Q.; Ji, J.; Tao, M.; Liu, Y.; You, Q.; Jiang, Z. Discovery of a Keap1-dependent peptide PROTAC to knockdown Tau by ubiquitination-proteasome degradation pathway. *Eur. J. Med. Chem.* **2018**, *146*, 251−259.
(26) Okamura, N.; Furumoto, S.; Fodero-Tavoletti, M. T.; Mulligan, R. S.; Harada, R.; Yates, P.; Pejoska, S.; Kudo, Y.; Masters, C. L.; Yanai, K.; Rowe, C. C.; Villemagne, V. L. Non-invasive assessment of Alzheimer's disease neurofibrillary pathology using 18F-THK5105 PET. *Brain* **2014**, *137* (6), 1762−1771.
(27) Tago, T.; Furumoto, S.; Okamura, N.; Harada, R.; Adachi, H.; Ishikawa, Y.; Yanai, K.; Iwata, R.; Kudo, Y. Preclinical Evaluation of [(18)F]THK-5105 Enantiomers: Effects of Chirality on Its Effectiveness as a Tau Imaging Radiotracer. *Mol. Imaging Biol.* **2016**, *18* (2), 258−66.
(28) Wiatrak, B.; Kubis-Kubiak, A.; Piwowar, A.; Barg, E. PC12 Cell Line: Cell Types, Coating of Culture Vessels, Differentiation and Other Culture Conditions. *Cells* **2020**, *9* (4), 958.
(29) Liu, Z.; Li, T.; Li, P.; Wei, N.; Zhao, Z.; Liang, H.; Ji, X.; Chen, W.; Xue, M.; Wei, J. The Ambiguous Relationship of Oxidative Stress, Tau Hyperphosphorylation, and Autophagy Dysfunction in Alzheimer's Disease. *Oxid Med. Cell Longev* **2015**, *2015*, 352723.
(30) Cai, L.; Li, R.; Tang, W. J.; Meng, G.; Hu, X. Y.; Wu, T. N. Antidepressant-like effect of geniposide on chronic unpredictable mild stress-induced depressive rats by regulating the hypothalamus-pituitary-adrenal axis. *Eur. Neuropsychopharmacol* **2015**, *25* (8), 1332−41.
(31) Hermans, S. J.; Nero, T. L.; Morton, C. J.; Gooi, J. H.; Crespi, G. A. N.; Hancock, N. C.; Gao, C.; Ishii, K.; Markulić, J.; Parker, M. W. Structural biology of cell surface receptors implicated in Alzheimer's disease. *Biophys Rev.* **2022**, *14* (1), 233−255.
(32) Piwowar, A.; Rembialkowska, N.; Rorbach-Dolata, A.; Garbiec, A.; Slusarczyk, S.; Dobosz, A.; Dlugosz, A.; Marchewka, Z.; Matkowski, A.; Saczko, J. Anemarrhenae asphodeloides rhizoma Extract Enriched in Mangiferin Protects PC12 Cells against a Neurotoxic Agent-3-Nitropropionic Acid. *Int. J. Mol. Sci.* **2020**, *21* (7), 2510.
(33) Yao, K.; Zhao, Y. F.; Zu, H. B. Melatonin receptor stimulation by agomelatine prevents Abeta-induced tau phosphorylation and oxidative damage in PC12 cells. *Drug Des Devel Ther* **2019**, *13*, 387−396.
(34) Liang, M.; Zheng, X.; Tu, L.; Ma, Z.; Wang, Z.; Yan, D.; Shen, Z. The liver-targeting study of the N-galactosylated chitosan in vivo and in vitro. *Artif Cells Nanomed Biotechnol* **2014**, *42* (6), 423−8.
(35) Huang, W.; Liang, M.; Li, Q.; Zheng, X.; Zhang, C.; Wang, Q.; Tang, L.; Zhang, Z.; Wang, B.; Shen, Z. Development of the "hidden" multifunctional agents for Alzheimer's disease. *Eur. J. Med. Chem.* **2019**, *177*, 247−258.

https://doi.org/10.1021/acsomega.2c02130
ACS Omega 2022, 7, 26308−26315